

**Supplementary Information**

**Pendant Conjugated Molecules based on Heterogeneous Core  
Structure with Enhanced Morphological and Emissive Properties for  
Organic Semiconductor Lasing**

Xu Liu,<sup>1,‡</sup> Ming Sang,<sup>1,‡</sup> Jinghan Zhou,<sup>1</sup> Shihao Xu,<sup>1</sup> Jialing Zhang,<sup>1</sup> Yu Yan,<sup>1</sup>

He Lin,<sup>1</sup> Wen-Yong Lai<sup>\*,1,2</sup>

<sup>1</sup>*Key Laboratory for Organic Electronics and Information Displays (KLOEID), Institute of Advanced Materials (IAM), Nanjing University of Posts & Telecommunications, 9 Wenyuan Road, Nanjing 210023, China*

<sup>2</sup>*Frontiers Science Center for Flexible Electronics (FSCFE), MIIT Key Laboratory of Flexible Electronics (KLoFE), Shaanxi Key Laboratory of Flexible Electronics, Xi'an Key Laboratory of Flexible Electronics, Xi'an Key Laboratory of Biomedical Materials & Engineering, Xi'an Institute of Flexible Electronics, Institute of Flexible Electronics (IFE), Northwestern Polytechnical University, Xi'an 710072, Shaanxi, China*

<sup>‡</sup>These authors contributed equally to this work.

\*Email: iamwylai@njupt.edu.cn

**General methods:** Commercial grade reagents were used without further purification unless otherwise stated. All the solvents for characterization were used after redistillation. THF was refluxed with sodium filament in the presence of benzophenone until a persistent violet-blue color appeared and then distilled. All reactions were monitored by thin layer chromatography (TLC) with silica gel 60 F254 (Merck, 0.2 mm). Column chromatography was carried out on silica gel (300-400 mesh).  $^1\text{H}$  NMR and  $^{13}\text{C}$  NMR spectra were recorded on a Bruker 400 plus at 295 K. The MALDI-TOF mass spectroscopy measurements were carried out with a Bruker mass spectrometer use trans-2-[3-(4-tert-Butylphenyl)-2-methyl-2-propenylidene]malononitrile as matrix. Elemental analysis was conducted with a Carlo Erba-1106 instrument. Differential scanning calorimetry (DSC) and thermo-gravimetric analysis (TGA) were done on Shimadzu DSC-60A and DTG-60H equipment for thermal analysis under a nitrogen atmosphere at a heating rate of  $10^\circ\text{C min}^{-1}$ , respectively. AFM measurements of surface morphology were conducted on the Bruker ScanAsyst AFM in auto scan (AC) mode. UV-Vis absorption spectra were recorded on a Shimadzu UV-3600 spectrophotometer. Fluorescence spectra were measured using a Shimadzu RF-5301PC spectrofluorimeter with a xenon lamp as the light source. The photoluminescence quantum yields (PLQYs) were determined by full-featured steady state/transient fluorescence spectrometer FLS-920 from Edinburgh Instruments. PL decays were measured with an Edinburgh FLS-920 spectrometer. All fluorescent lifetimes were determined from the data using the Edinburgh Instruments software package. The powder wide-angle X-ray diffraction (WAXD) measurements were carried out with a Bruker D8 Advance diffractometer with Cu radiation ( $\lambda_1 = 1.54056 \text{ \AA}$ ,  $\lambda_2 = 1.54439 \text{ \AA}$ ) at 40 kV and 40 mA equipped with a Linkseye detector. Measurements were collected within a  $2\theta$  range from  $5^\circ$  to  $50^\circ$  with a step size of  $0.2^\circ$ . Cyclic voltammetry (CV) was performed on an Eco Chemie's Autolab at room temperature under nitrogen with a scanning rate of  $100 \text{ mV/s}$ , which used a standard three-electrode electrochemical cell in

nonaqueous acetonitrile solution with 0.1 M tetra-*n*-butylammonium hexafluorophosphate (Bu<sub>4</sub>NPF<sub>6</sub>). The HOMO levels are calculated according to the equations ( $E_{\text{HOMO}} = -[E_{\text{ox}} - E(\text{Fc}/\text{Fc}^+) + 4.8]$  eV,  $E_{\text{ox}}(\text{Fc}/\text{Fc}^+) = 0.08$  eV). The ASE measurements in films were optically pumped by an Nd:YAG laser (a repetition rate of 10 Hz, a pulse duration of 12 ns) with the excitation laser source at their absorption maxima. The ASE measurements were conducted in air. The third harmonic (355 nm, 10 ns) of a Q-switched Nd:YAG laser was used to pump the film at a repetition rate of 10 Hz after being focused into a narrow stripe by a cylindrical lens. The pump laser energy was adjusted by calibrated neutral density filters and the emissions were subsequently collected from the tip area. The edged emission was collected and analyzed by means of a fiber-coupled spectrograph and charge-coupled device (CCD) detector. During the test, the stripe length was maintained, but the stripe was removed from the edge of the film. Given that the emission from the end of the pump stripe ( $I_0$ ) was constant, the emission from the edge of the film should be reduced based on the equation:  $I(\lambda) = I_0(\lambda) \exp(-\alpha(\lambda) \times x)$ , where  $x$  is the length of the non-pumped region between the excitation region and the film edge and  $\alpha$  is the loss coefficient. By fitting the ASE intensity at various stripe locations as a function of  $x$  with the equation as mentioned before, the plot of loss coefficient versus stripe position was obtained. Ground-state geometries of the molecular structures were optimized at the B3LYP functional level with the 6-31G (d, p) basis set supplemented with polarization functions (Figure 9, Table 3).

## Experimental Section

Commercially available chemicals were used as received. All reactions were monitored using thin layer chromatography (TLC) with silica gel 60 F254 (Merck, 0.2 mm). Column chromatography was carried out on silica gel (300–400 mesh). <sup>1</sup>H NMR and <sup>13</sup>C NMR spectra were recorded on a Bruker 400 plus at 295 K. The MALDI-TOF mass spectroscopy measurements were carried out using a

Bruker mass spectrometer. Differential scanning calorimetry (DSC) and thermo-gravimetric analysis (TGA) were carried out on Shimadzu DSC-60A and DTG-60H equipment, respectively. UV-Vis absorption spectra were recorded on a Shimadzu UV-3600 spectrophotometer. Fluorescence spectra were measured using a Shimadzu RF-5301PC spectrofluorimeter with a xenon lamp as the light source.

### **Device Fabrication and Measurements:**

Thin-film samples (110 nm thickness for **C1** film and 97 nm for **C2** film) for optical measurements (absorption and PL spectra, PLQY, PL decay, and ASE measurements) were prepared by spin-coating starburst solutions (comprising 35 mg mL<sup>-1</sup> of **C1** or 20 mg mL<sup>-1</sup> of **C2** in CHCl<sub>3</sub>) onto precleaned spectrosil substrates.

For ASE measurements, the samples were optically pumped with the pulsed (5 ns, 10 Hz, 355 nm) output of a Q-switched Nd:YAG laser pumped optical parametric amplifier (Spectron SL450) focused with a cylindrical lens to form a 4 mm × 0.55 mm stripe-shaped excitation area on the sample. The wavelength of excitation light was determined based on the absorption of the films. The ASE measurements were not corrected with the Abs of the films at the laser excitation wavelength, and the pump energy density is the direct value of the laser excitation.

### **Synthesis and characterization**

All reactions and manipulations were operated under nitrogen atmosphere. All the reagents used were purchased from commercial suppliers (from Sigma-Aldrich, J&K or Xiya Reagent (China), and so on.) and used without further purification unless otherwise stated.

#### **6-(2,7-dibromo-9H-carbazol-9-yl)-N<sup>2</sup>,N<sup>2</sup>,N<sup>4</sup>,N<sup>4</sup>-tetraphenyl-1,3,5-triazine-2,4-diamine (DBrCzDPAT) (2):**

Diphenylamine (0.42 g, 2.5 mmol) was dissolved in dry THF (10 mL) under nitrogen in a two-necked,

round-bottom flask. *n*-Buthyllithium (2.5M in hexane solution) (1.1 mL, 2.7 mmol) was added dropwise to the diphenylamine solution and the mixture was stirred for 30 min. In a separate two-necked, round-bottom flask, **1** (0.47 g, 1 mmol) was dissolved in dry THF (30 mL) in a nitrogen atmosphere. The diphenylamine lithium solution was added dropwise to the **1** solution by using a syringe within 10 min. The reaction mixture was refluxed for 12 h. After the solution was cooled to room temperature, 50 mL water was added. The product was filtered off, washed with water, hexane and acetone, and further purified by hot filtration from dichloromethane and ethanol, to yield 0.42 g (57%) of **2** as a white solid. MALDI-TOF MS (*m/z*): Calcd for C<sub>39</sub>H<sub>26</sub>Br<sub>2</sub>N<sub>6</sub>, Exact Mass: 736.06, Mol. Wt.: 738.49; Found: 736.50. <sup>1</sup>H NMR (400 MHz, CDCl<sub>3</sub>): δ 8.32 (d, *J* = 1.5 Hz, 2H), 7.68 (d, *J* = 8.2 Hz, 2H), 7.33 (dd, *J* = 8.2, 1.6 Hz, 22H). <sup>13</sup>C NMR (100 MHz, CDCl<sub>3</sub>): δ 166.2, 164.3, 143.2, 139.8, 129.1, 127.6, 126.2, 124.1, 120.9, 120.5, 119.8.

**General procedure for the synthesis of Cx:** To a stirred solution of compound (**2**) (0.37 g, 0.5 mmol) in toluene (45 mL) was added oligofluorene boronate (1.3 mmol), potassium carbonate (0.36 g, 2.6 mmol), H<sub>2</sub>O (15 mL), and Pd(PPh<sub>3</sub>)<sub>4</sub> (35 mg, 0.031 mmol). The resulting mixture was stirred at 100°C under nitrogen atmosphere for 24 h. The solvent was evaporated under reduced pressure and the residue was treated with water (80 mL), extracted with dichloromethane. The organic layers were combined and washed twice with water and once with brine, dried over anhydrous magnesium sulfate. After removing the solvent under reduced pressure, the residue was purified by column chromatography to produce **Cx**.

**6-(2,7-bis(9,9-dihexyl-9H-fluoren-2-yl)-9H-carbazol-9-yl)-N<sup>2</sup>,N<sup>2</sup>,N<sup>4</sup>,N<sup>4</sup>-tetraphenyl-1,3,5-triazine-2,4-diamine (C1)**

White solid, yield 79%. m. p. = 238 °C. MALDI-TOF MS (*m/z*): Calcd for C<sub>89</sub>H<sub>92</sub>N<sub>6</sub>, Exact Mass:

1244.74, Mol. Wt.: 1245.76; Found: 1245.19.  $^1\text{H}$  NMR (400 MHz,  $\text{CDCl}_3$ ):  $\delta$  8.55 (d,  $J = 0.9$  Hz, 2H), 8.03 (d,  $J = 8.0$  Hz, 2H), 7.81 (d,  $J = 7.3$  Hz, 2H), 7.71 (d,  $J = 7.8$  Hz, 2H), 7.56 – 7.47 (m, 4H), 7.44 – 7.24 (m, 16H), 7.08 (t,  $J = 8.0$  Hz, 10H), 6.91 (s, 2H), 2.11 – 2.00 (m, 8H), 1.17 – 1.05 (m, 24H), 0.78 (t,  $J = 6.9$  Hz, 20H).  $^{13}\text{C}$  NMR (100 MHz,  $\text{CDCl}_3$ ):  $\delta$  166.2, 164.3, 151.0, 143.3, 141.5, 141.0, 140.7, 140.0, 139.8, 128.6, 127.6, 127.1, 126.9, 126.8, 125.8, 124.5, 122.9, 122.4, 122.0, 119.9, 119.6, 119.1, 115.8, 55.1, 31.5, 29.8, 23.9, 22.6, 14.0. Anal. Calcd for  $\text{C}_{89}\text{H}_{92}\text{N}_6$ : C, 85.81; H, 7.44; N, 6.75. Found: C, 86.03; H, 7.35; N, 6.79.

**6-(2,7-bis(9,9,9',9'-tetrahexyl-9H,9'H-[2,2'-bifluoren-7-yl)-9H-carbazol-9-yl)- $\text{N}^2,\text{N}^2,\text{N}^4,\text{N}^4$ -tetraphenyl-1,3,5-triazine-2,4-diamine (C2):** White solid, yield 45%. m. p. = 256 °C. MALDI-TOF MS ( $m/z$ ): Calcd for  $\text{C}_{139}\text{H}_{156}\text{N}_6$ , Exact Mass: 1909.24, Mol. Wt.: 1910.77; Found: 1909.70.  $^1\text{H}$  NMR (400 MHz,  $\text{CDCl}_3$ ):  $\delta$  8.56 (s, 2H), 8.04 (d,  $J = 8.0$  Hz, 2H), 7.88 (d,  $J = 7.8$  Hz, 2H), 7.81 (d,  $J = 7.8$  Hz, 2H), 7.78 – 7.64 (m, 12H), 7.57 (s, 2H), 7.52 (d,  $J = 8.1$  Hz, 2H), 7.39 – 7.28 (m, 14H), 7.10 (dd,  $J = 14.7, 7.5$  Hz, 10H), 6.91 (s, 4H), 2.12 (t,  $J = 7.8$  Hz, 8H), 2.05 (m, 8H), 1.16-1.08 (m, 48H), 0.88 (d,  $J = 7.8$  Hz, 8H), 0.78-0.76 (m, 32H).  $^{13}\text{C}$  NMR (100 MHz,  $\text{CDCl}_3$ ):  $\delta$  166.2, 164.4, 151.8, 151.4, 151.3, 151.0, 143.3, 141.5, 140.8, 140.7, 140.5, 140.5, 140.3, 140.1, 140.0, 139.4, 128.6, 127.6, 126.8, 126.0, 124.6, 122.9, 122.1, 121.4, 119.9, 119.7, 119.1, 115.8, 55.2, 55.18, 40.4, 40.3, 31.5, 31.4, 29.8, 29.7, 22.6, 22.5, 14.0. Anal. Calcd for  $\text{C}_{139}\text{H}_{156}\text{N}_6$ : C, 87.37; H, 8.23; N, 4.40. Found: C, 87.11; H, 8.28; N, 4.29.

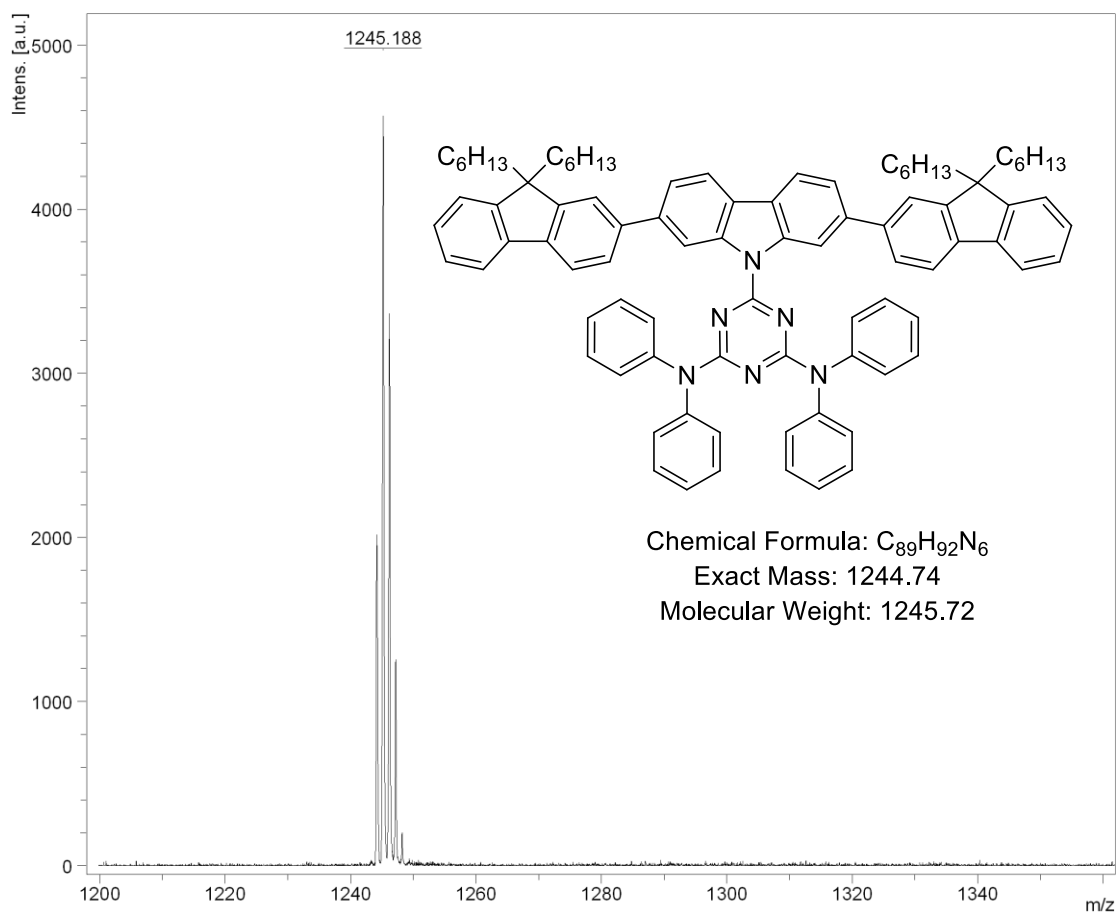


**Figure S1.** MALDI-TOF mass spectra of C1.

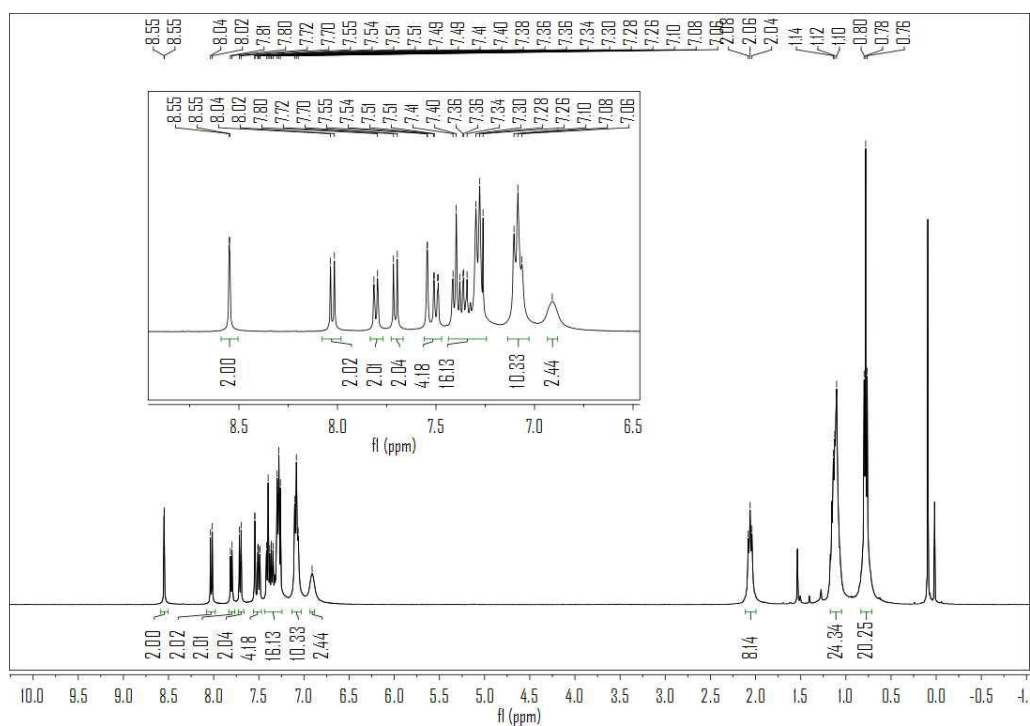


**Figure S2.**  $^1H$  NMR spectra of C1

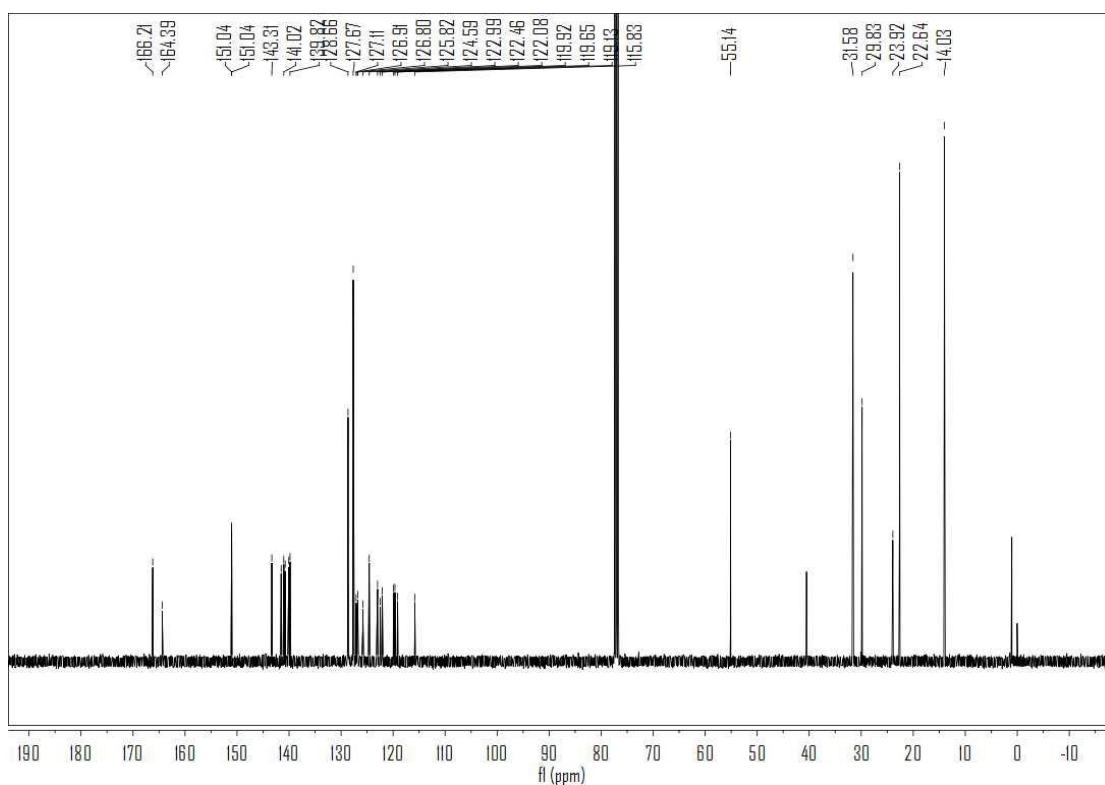


**Figure S3.**  $^{13}\text{C}$  NMR spectra of **C1**.

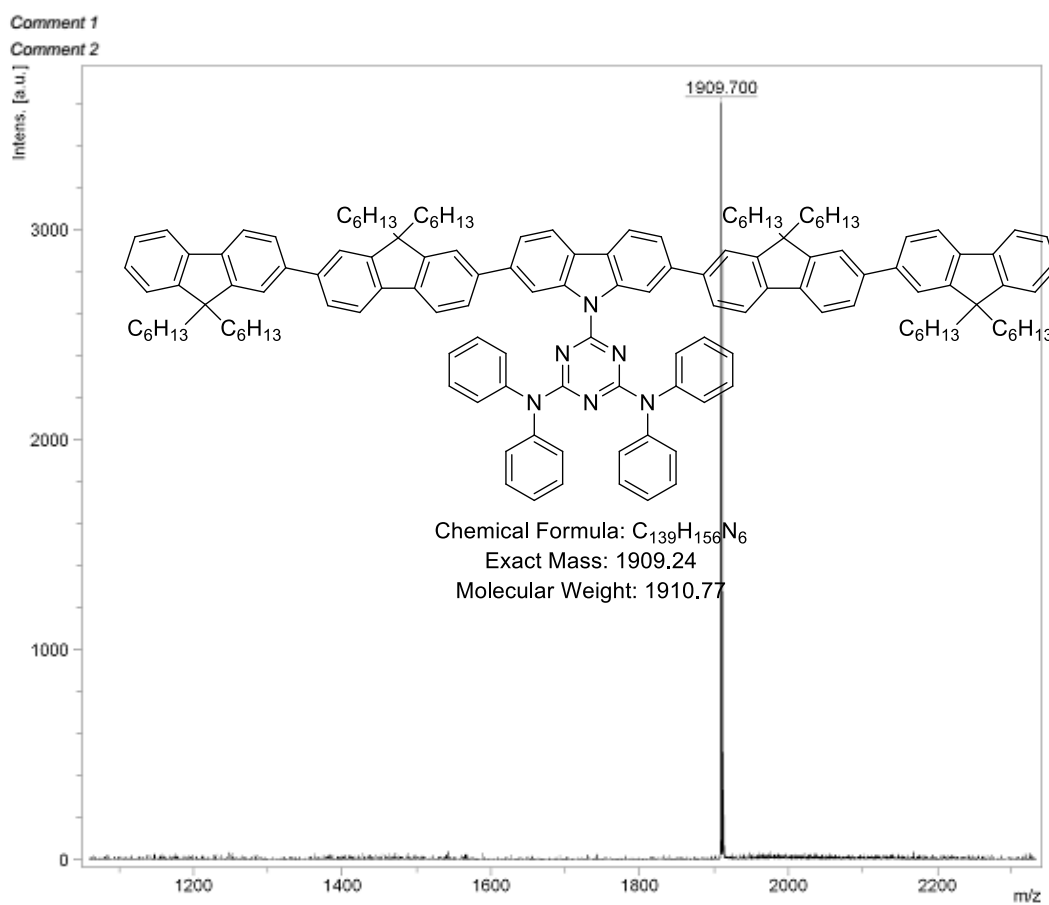


**Figure S4.** MALDI-TOF mass spectra of **C2**.

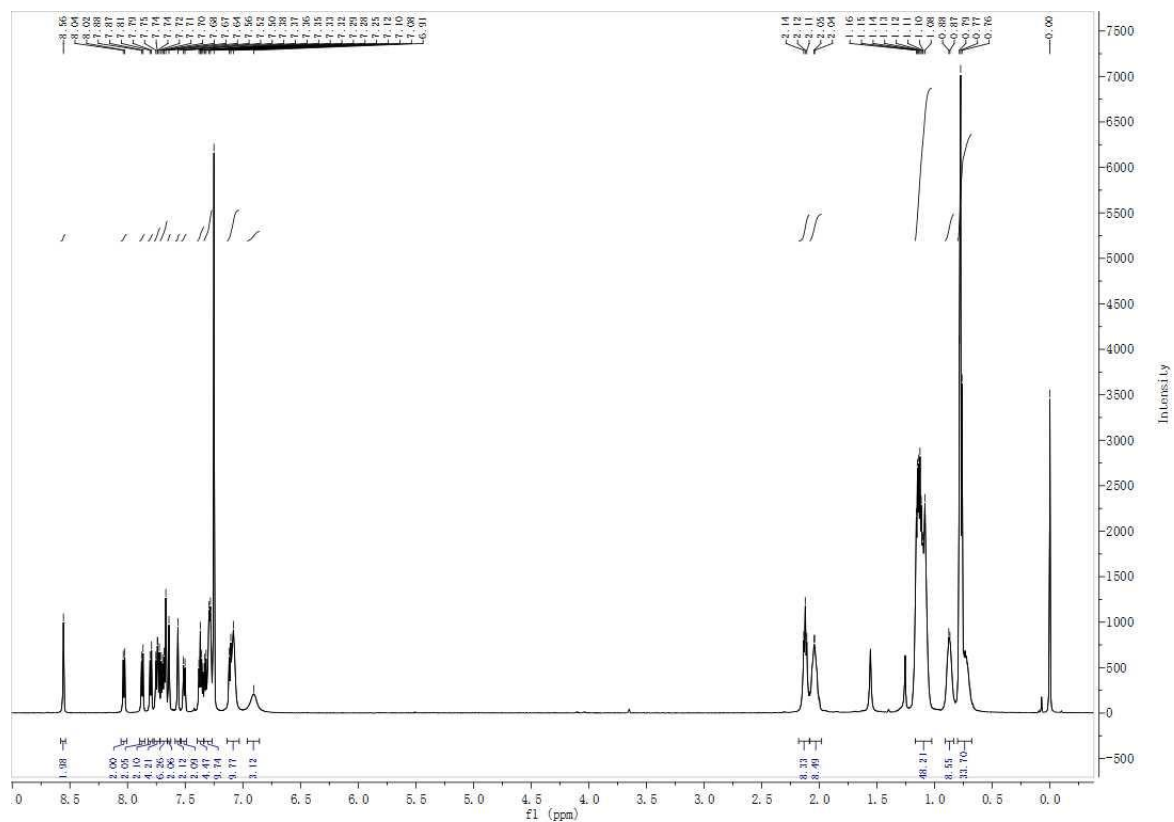


Figure S5.  $^1\text{H}$  NMR spectra of C2

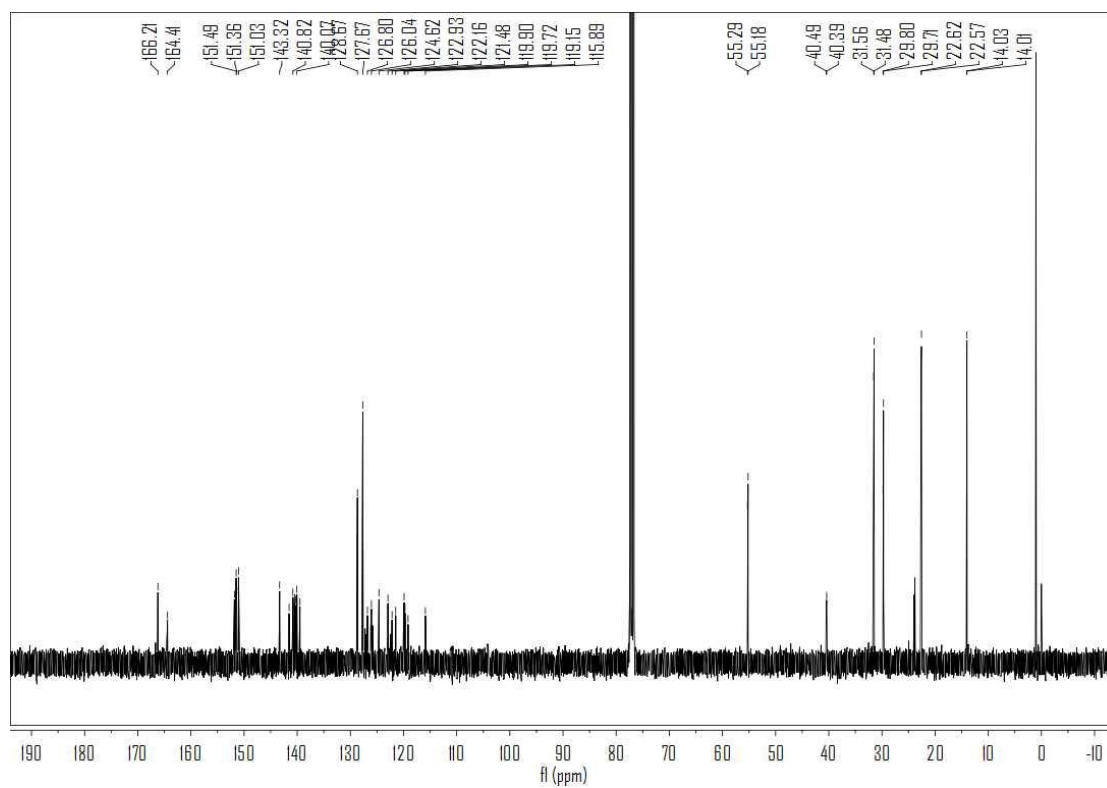
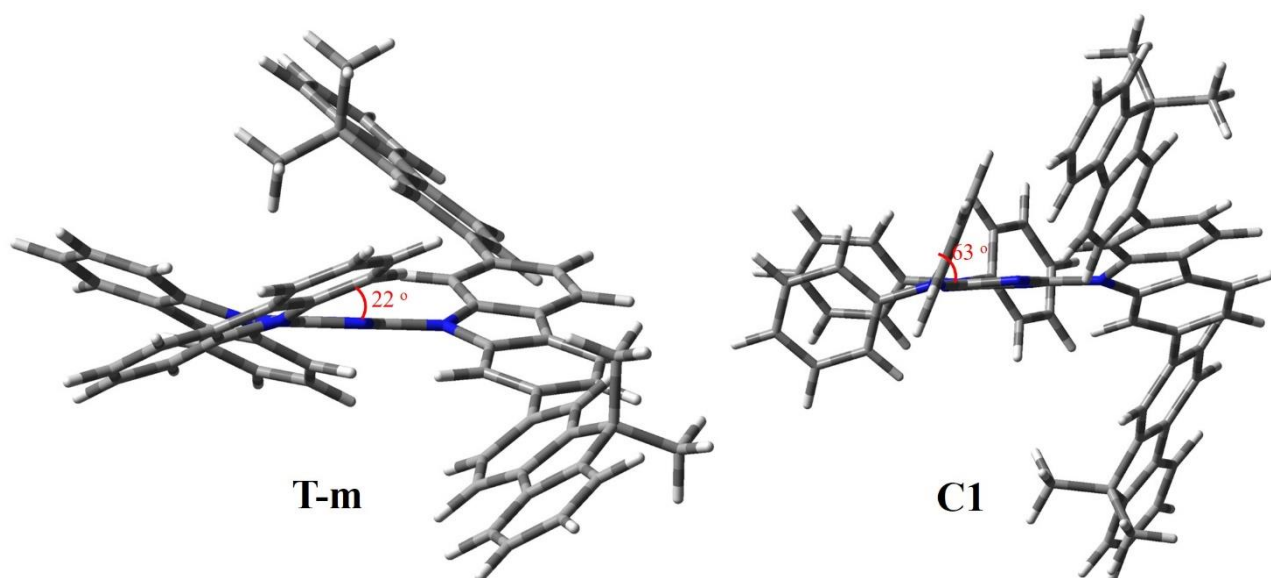
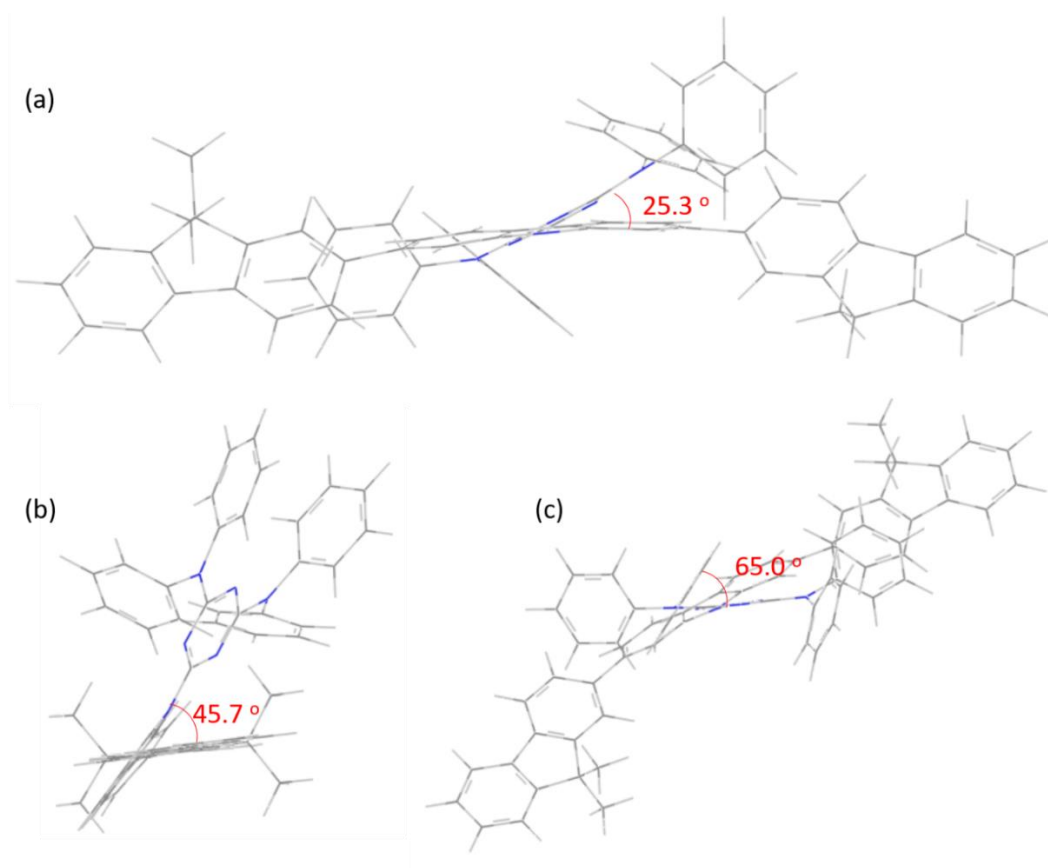


Figure S6.  $^{13}\text{C}$  NMR spectra of C2.



**Figure S7.** The dihedral angle between the phenyl units of DPA or carbazole and triazine in **T-m** and **C1**.



**Figure S8.** The dihedral angle between (a) the carbazole and triazine, (b) carbazole and fluorene, (c) phenyl units of carbazole and triazine in **C1**, respectively.

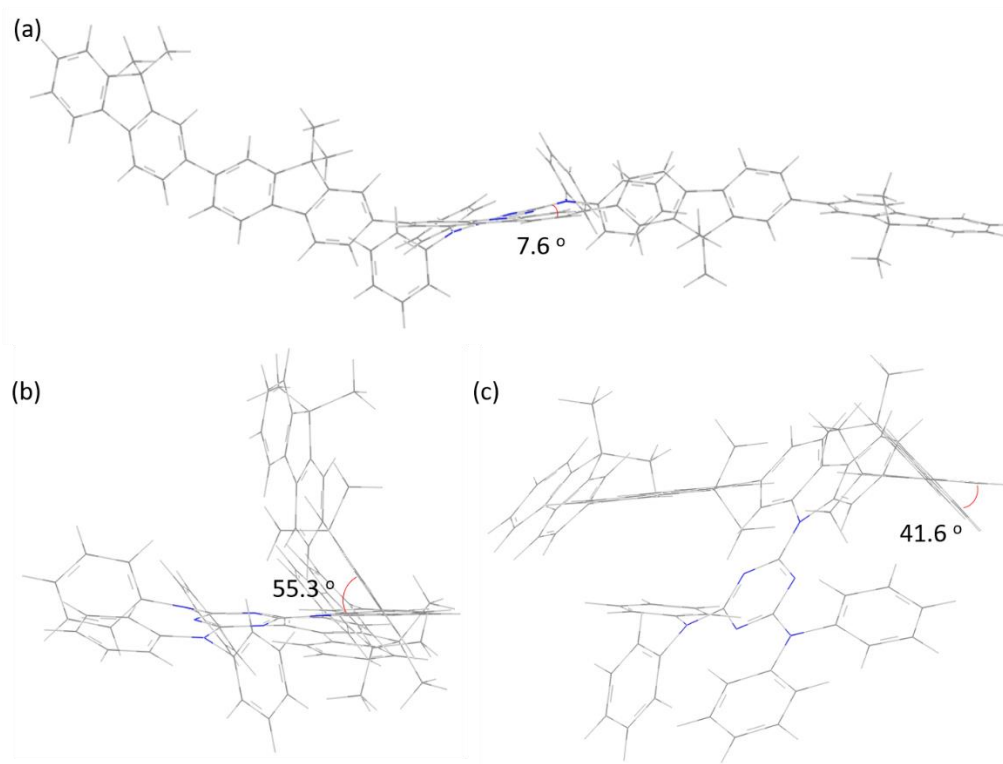


**Figure S9.** The dihedral angle between (a) the carbazole and triazine, (b) carbazole and fluorene, (c) fluorene and fluorene in **C2**, respectively.

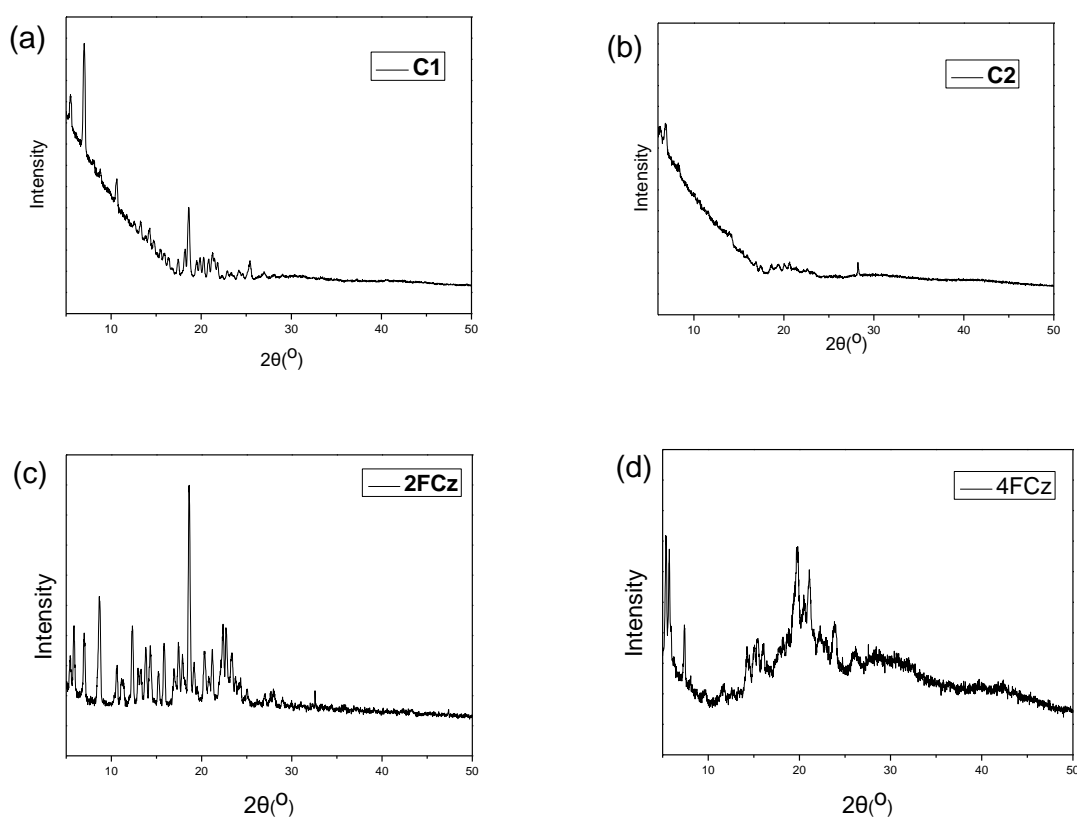


**Figure S10.** Wide-angle X-ray diffraction (WAXD) patterns of **Cx** and **xFCz** in powders.

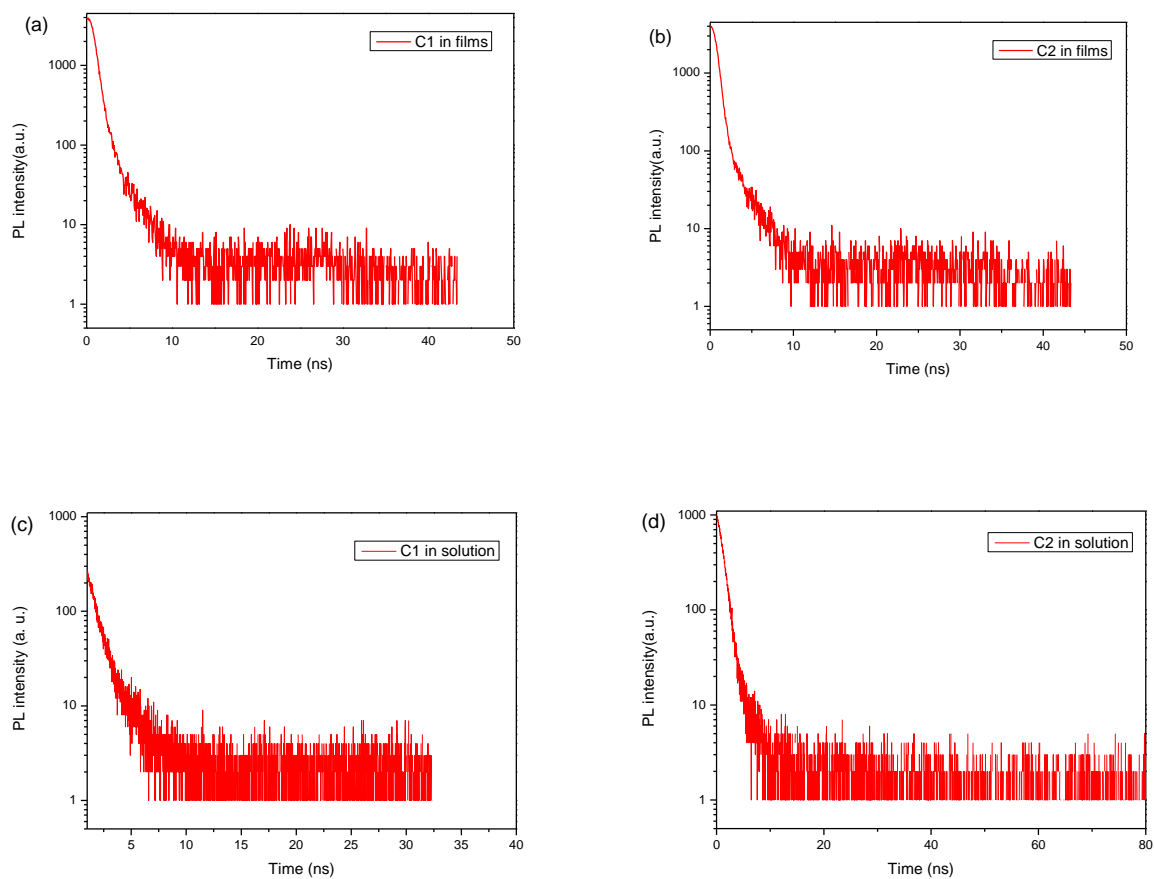


**Figure S11.** Fluorescence decay of (a) **C1** and (b) **C2** in films, (c) **C1** and (d) **C2** in solutions.

**Table S1.** Glass Transition Temperatures and Thermal Stability of **CX** and **XFCz**.

Compound	$T_d$ [°C] (TGA, 5% mass loss)	$T_g$ [°C]
<b>2FCz</b>	393	64
<b>4FCz</b>	374	NA
<b>C1</b>	426	NA
<b>C2</b>	405	NA

<sup>[a]</sup> Measured at 10°C/min.

**Table S2.** ASE Properties of **XFCz** and **CX**.

Compound	$\lambda_{\text{ASE}}^a$ (nm)	$E_{\text{th}}^{\text{ASE}}$ ( $\mu\text{J}/\text{cm}^2$ )	FWHM <sup>b</sup> (nm)
<b>C1</b>	417	5.0	4.3
<b>C2</b>	436	5.0	4.9
<b>2FCz</b>	427	5.0	3.5
<b>4FCz</b>	446	6.3	5.2

<sup>a</sup>ASE peak wavelength. <sup>b</sup>Minimal full width at half-maximum of the ASE band.

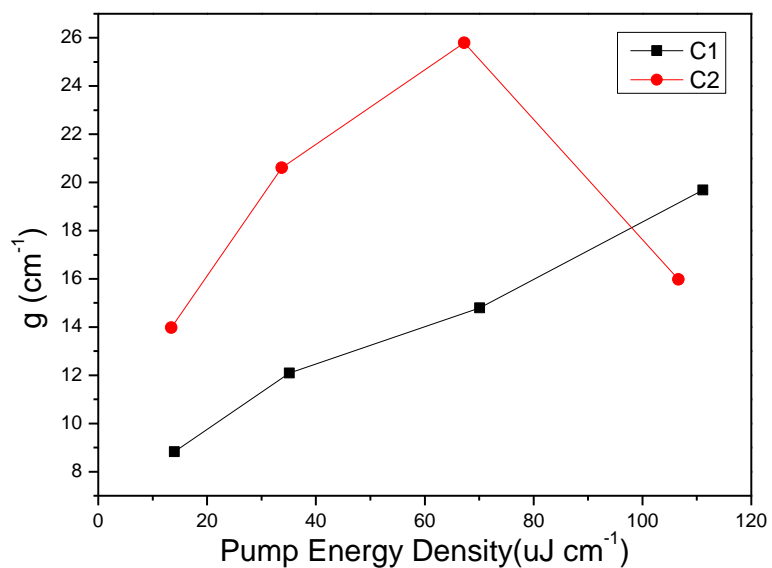


**Figure S12.** The plot of net gain coefficients ( $g$ ) as a function of different pumping intensity for **C1** and **C2**.